CARDIAC HYPERTROPHY

Long noncoding RNA *Chast* promotes cardiac remodeling

Janika Viereck,[1,2]* Regalla Kumarswamy,[1]* Ariana Foinquinos,[1]* Ke Xiao,[1] Petros Avramopoulos,[3,4] Meik Kunz,[5] Marcus Dittrich,[5,6] Tobias Maetzig,[7] Karina Zimmer,[1] Janet Remke,[1] Annette Just,[1] Jasmin Fendrich,[1] Kristian Scherf,[1] Emiliano Bolesani,[8] Axel Schambach,[7] Frank Weidemann,[9,10] Robert Zweigerdt,[8] Leon J. de Windt,[11] Stefan Engelhardt,[3,4] Thomas Dandekar,[5] Sandor Batkai,[1] Thomas Thum[1,2,12†]

Recent studies highlighted long noncoding RNAs (lncRNAs) to play an important role in cardiac development. However, understanding of lncRNAs in cardiac diseases is still limited. Global lncRNA expression profiling indicated that several lncRNA transcripts are deregulated during pressure overload–induced cardiac hypertrophy in mice. Using stringent selection criteria, we identified *Chast* (cardiac hypertrophy–associated transcript) as a potential lncRNA candidate that influences cardiomyocyte hypertrophy. Cell fractionation experiments indicated that *Chast* is specifically up-regulated in cardiomyocytes in vivo in transverse aortic constriction (TAC)–operated mice. In accordance, *CHAST* homolog in humans was significantly up-regulated in hypertrophic heart tissue from aortic stenosis patients and in human embryonic stem cell–derived cardiomyocytes upon hypertrophic stimuli. Viral-based overexpression of *Chast* was sufficient to induce cardiomyocyte hypertrophy in vitro and in vivo. GapmeR-mediated silencing of *Chast* both prevented and attenuated TAC-induced pathological cardiac remodeling with no early signs on toxicological side effects. Mechanistically, *Chast* negatively regulated Pleckstrin homology domain–containing protein family M member 1 (opposite strand of *Chast*), impeding cardiomyocyte autophagy and driving hypertrophy. These results indicate that *Chast* can be a potential target to prevent cardiac remodeling and highlight a general role of lncRNAs in heart diseases.

INTRODUCTION

Diseases of the cardiovascular system are the most common cause of human morbidity and mortality in the world. Exposure of the heart to different stressors leads to "cardiac remodeling" with detrimental outcomes. At the cellular level, a hallmark of the remodeling process is pathological cardiomyocyte hypertrophy. Prolonged hypertrophic growth of the heart results in heart failure and often death of the affected individual (*1*). Despite advances in pharmacologic treatment of cardiac remodeling by β blockers, angiotensin-converting enzyme inhibitors, and mineralocorticoid receptor blockers, the prognosis of affected individuals remains poor.

The human genome is tremendously larger than that of more simple organisms such as worms, although it has a comparable number of protein-regulating genes. All protein-coding genes originate from about only 1.5% of the genome, and the larger remaining portion of the genome remains either untranscribed or (more often) transcribed to noncoding RNAs (*2*), of which functional importance is still less understood. Long noncoding RNAs (lncRNAs) are a class of noncoding RNAs that are larger than 200 nucleotides (nt) and do not generally encode proteins. LncRNAs regulate pathways by diverse mechanisms including chromatin modification (*3*), transcriptional (*4*) and posttranscriptional regulation (*5*), and influencing subcellular trafficking (*6*, *7*). The role of lncRNAs in the heart has just begun to be uncovered. LncRNA *Braveheart* (*Bvht*) was recently shown to be crucial for cardiac development in mice (*8*), whereas another lncRNA, *Fendrr*, was able to control chromatin modifications and, thus, developmental signaling in the rodent heart (*9*). LncRNAs have demonstrated functional roles in the adult murine cardiac system and in human cardiovascular cells (*10*–*12*), and have strong prognostic potential as biomarkers in heart failure patients (*13*).

Thus, here, we generated a whole-genome lncRNA profile to identify differentially expressed lncRNAs in hypertrophic mouse hearts. Subsequent functional studies revealed that lncRNA ENSMUST00000130556, which we have named cardiac hypertrophy–associated transcript (*Chast*), plays an important role in the pathogenesis of pressure overload–induced cardiac remodeling. Mechanistically, *Chast* impedes expression of the autophagy regulator Pleckstrin homology domain–containing protein family M member 1 (*Plekhm1*), and its silencing results in autophagic inhibition and cardiomyocyte hypertrophy. Suppression of *Chast* before and after induction of hypertrophy prevented or attenuated established disease, respectively, indicating the potential for lncRNAs as new therapeutic targets in cardiovascular diseases.

RESULTS

LncRNA expression pattern is altered during cardiac pressure overload in mice

To investigate lncRNA transcriptome changes during pressure overload–induced cardiac hypertrophy, we performed a lncRNA microarray

[1]Institute of Molecular and Translational Therapeutic Strategies (IMTTS), Integriertes Forschungs- und Behandlungszentrum Transplantation (IFB-Tx), Hannover Medical School, D-30625 Hannover, Germany. [2]Excellence Cluster REBIRTH, Hannover Medical School, D-30625 Hannover, Germany. [3]Institute of Pharmacology and Toxicology, Technical University of Munich, D-80802 Munich, Germany. [4]German Center for Cardiovascular Research (DZHK), partner site Munich Heart Alliance, D-80802 Munich, Germany. [5]Department of Bioinformatics, University of Würzburg, D-97074 Würzburg, Germany. [6]Institute of Human Genetics, University of Würzburg, D-97074 Würzburg, Germany. [7]Institute of Experimental Hematology, Hannover Medical School, D-30625 Hannover, Germany. [8]Leibniz Research Laboratories for Biotechnology and Artificial Organs (LEBAO), Department of Cardiac, Thoracic, Transplantation and Vascular Surgery, Hannover Medical School, D-30625 Hannover, Germany. [9]Department of Cardiology, Julius-Maximilians University, D-97080 Würzburg, Germany. [10]Comprehensive Heart Failure Center, University of Würzburg, D-97078 Würzburg, Germany. [11]Department of Cardiology, Maastricht University, 6202 AZ Maastricht, Netherlands. [12]National Heart and Lung Institute, Imperial College London, SW3 6NP London, UK.
*These authors contributed equally to this work.
†Corresponding author. E-mail: thum.thomas@mh-hannover.de

analysis in RNA isolated from sham or transverse aortic constriction (TAC)–operated mouse hearts (Fig. 1A). Most lncRNAs represented on the array (19,427 of 31,423 lncRNAs) were detected, and several lncRNAs were deregulated in hypertrophic hearts (Fig. 1B): 1237 lncRNAs were up-regulated after TAC, whereas 1623 lncRNAs were down-regulated. To avoid detection of primary mRNA in quantitative polymerase chain reaction (qPCR), we excluded lncRNA transcripts that were located within a protein-coding gene in sense orientation. Next, we selected 22 highly deregulated (11 up-regulated, 11 down-regulated with fold changes >3) candidates for validation. Of these 22 candidates, transcripts were consistently detected in all tested samples (n = 5 mice per group) for 13 lncRNAs (six up-regulated and seven down-regulated). qPCR analyses indicated that four lncRNAs were significantly deregulated (one up-regulated and three down-regulated) in TAC-operated hearts (Fig. 1C).

From the three down-regulated, two showed protein-coding potential (ENSMUST00000019980 and ENSMUST00000046048, but not AK083183). We nevertheless focused on the up-regulated lncRNAs, specifically ENSMUST00000130556 (Fig. 1, B and C), because of our interest in developing inhibitory oligonucleotide drugs as a therapeutic approach. Herein, we refer to this lncRNA as *Chast*. Expression of *Chast* was temporally regulated between 4 and 13 weeks after left ventricular (LV) pressure overload in mice, with a peak expression level at 6 weeks (Fig. 1D). At this time point (4 to 6 weeks after initiation of TAC-mediated LV pressure overload), compensated cardiac function turns toward decompensation, for example, normal cardiac function started to decrease (Fig. 1D). Cellular fractionation experiments revealed that *Chast* was specifically up-regulated in cardiomyocytes (rather than in fibroblasts) of 6-week TAC-operated murine hearts (Fig. 1E).

We performed 3′ and 5′ RACE experiments in RNA isolated from mouse hearts and confirmed that *Chast* is expressed in heart tissue as a single, full-length, 823-nt transcript with two exons (Fig. 1F). This validated sequence of *Chast* strongly correlates to the sequence information of transcript ENSMUST00000130556 annotated by Ensembl (depicted in red) but harbors a transcription start site located 100 nt downstream of the annotated transcript (Fig. 1F, depicted in blue). Furthermore, the *Chast* gene partially overlaps in antisense to the protein

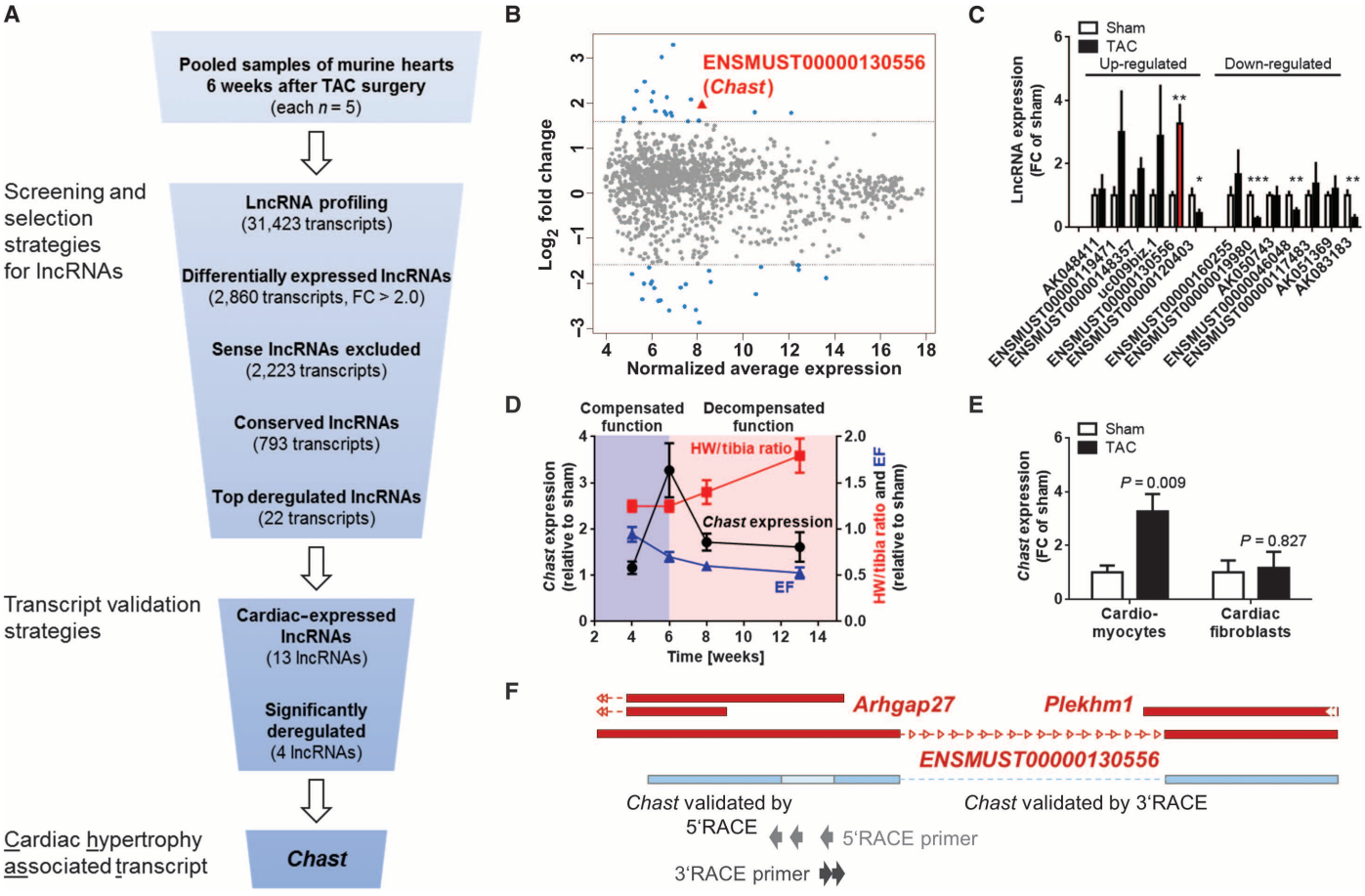

Fig. 1. *Chast* is induced by pressure overload in mice. (**A**) Selection strategy of TAC-induced murine lncRNAs derived from microarray-based profiling. (**B**) MA plot (M, log ratio; A, average mean) of differentially regulated lncRNAs [fold change (FC) > 1.5 indicated by symbols, signs, and dashed line; *Chast* is highlighted in red]. (**C**) Validation of deregulated lncRNAs induced by TAC. *Chast* is highlighted in red. Data are mean FC relative to sham ± SEM (n = 6 animals per group). *P < 0.05; **P < 0.01; ***P = 0.001 versus respective sham, Student's t test. (**D**) Time course of *Chast* expression compared to heart weight–to–tibia length ratio and ejection fraction (EF), each relative to sham controls. Data are means ± SEM (n = 5 to 8 animals). HW, heart weight. (**E**) *Chast* expression in heart cell fractions after TAC (n = 6). Data are mean FC relative to sham ± SEM. P values versus sham determined by Student's t test. (**F**) Graphical representation of 3′ and 5′ rapid amplification of cDNA (complementary DNA) ends (RACE).

coding genes Rho GTPase (guanosine triphosphatase) activating protein 27 (*Ahrgap27*) and *Plekhm1*.

To confirm that *Chast* is a noncoding RNA, the protein-coding potential of the full-length transcript was analyzed using the Protein Coding Potential Calculator (*14*). Similar to other bona fide murine lncRNAs *Xist*, *Bvht*, and *Fendrr*, *Chast* received low coding-potential scores. Known protein-coding genes *Gapdh*, β-actin (*Actb*), α-MHC (*Myh6*), and troponin T (*Tnnt2*) served as positive controls (fig. S1A). Further, we applied the sequence frame translator and the NCBI (National Center for Biotechnology Information) open reading frame (ORF) finder and identified four open reading frames that were small (<100 amino acids) (fig. S1B). To rule out the possibility that *Chast* encodes one of these peptides, we overexpressed the transcript in murine HL-1 atrial cardiomyocytes and analyzed the resulting peptides by high-resolution mass spectrometry. None of the peptides corresponding to potential ORFs were identified (fig. S1B).

Chast induces cardiomyocyte hypertrophy

Expression of *Chast* was induced upon stimulation of HL-1 cardiomyocytes with the prohypertrophic factors phenylephrine (PE) and isoproterenol (ISO) (Fig. 2A). Lentiviral overexpression of *Chast* induced hypertrophic growth in HL-1 cells (Fig. 2, B and C). Silencing of *Chast* with GapmeRs—antisense oligonucleotides containing a central DNA complementary to its target and flanked by blocks of locked nucleic acids, which forms a stable DNA/RNA heteroduplex that provoke ribonuclease H (RNase H)–mediated target degradation—significantly attenuated PE + ISO–induced hypertrophic response in HL-1 cells (Fig. 2, E and F). Consistently, expression of the cardiac stress marker atrial natriuretic peptide (*Anp*) was increased either by PE + ISO treatment or upon *Chast* overexpression, whereas GapmeR-mediated suppression of *Chast* prevented PE + ISO–induced *Anp* expression (Fig. 2, D and G). These results indicate that *Chast* is involved in prohypertrophic growth of cultured cardiomyocytes.

Chast is activated by NFAT signaling and acts as a regulator of hypertrophic genes and pathways

Bioinformatic analysis revealed that the gene encoding *Chast* has at least one binding site for the prohypertrophic transcription factor NFAT (nuclear factor of activated T cells) (Fig. 3A and table S1). To test if the expression of *Chast* is regulated by NFAT, we treated murine HL-1 cardiomyocytes with the pharmacological NFAT inhibitor 11R-VIVIT. Upon NFAT inhibition, expression of *Chast*, along with another known NFAT target *Mcip1.4*, was significantly down-regulated (Fig. 3B). To determine whether *Chast* is regulated by NFAT activation, we tested *Chast* expression in hearts of calcineurin (Myh6-*CnA*) transgenic (TG) mice (*15*), where NFAT is constitutively active. Calcineurin TG mice displayed high *Mcip1.4* levels and an approximately threefold increase in *Chast* expression compared with wild-type animals (Fig. 3C). Binding of NFAT to the *Chast* promoter was verified by chromatin immunoprecipitation (ChIP) assays (Fig. 3D).

To delineate a potential mechanism of action, we measured *Chast* expression in RNA extracted from different cellular compartments of mouse HL-1 cardiomyocytes. As expected, *Gapdh* and *ActB* were predominantly found in cytosol, whereas known epigenetic modulators, such as *Xist* and *Neat1* lncRNAs, were predominantly found associated with chromatin. *Chast* was found to be ubiquitously present

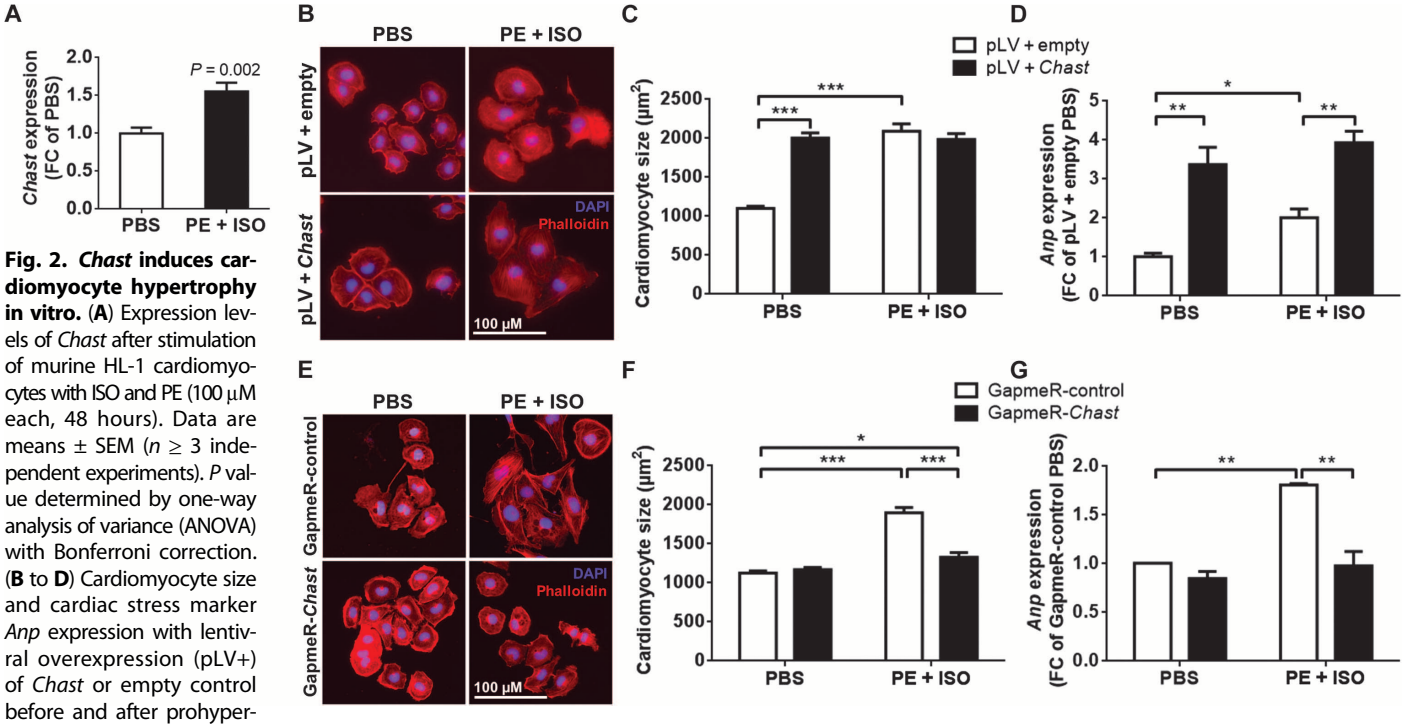

Fig. 2. *Chast* induces cardiomyocyte hypertrophy in vitro. (**A**) Expression levels of *Chast* after stimulation of murine HL-1 cardiomyocytes with ISO and PE (100 μM each, 48 hours). Data are means ± SEM ($n \geq 3$ independent experiments). *P* value determined by one-way analysis of variance (ANOVA) with Bonferroni correction. (**B** to **D**) Cardiomyocyte size and cardiac stress marker *Anp* expression with lentiviral overexpression (pLV+) of *Chast* or empty control before and after prohypertrophic (PE + ISO) treatment. (**E** to **G**) Cardiomyocyte size and *Anp* expression upon GapmeR-mediated silencing of *Chast* before and after prohypertrophic (PE + ISO) treatment. GapmeR-control was a scrambled sequence. In (C), (D), (F), and (G), data are mean FC relative to control ± SEM ($n \geq 3$ independent experiments). $^{*}P < 0.05$; $^{**}P < 0.01$; $^{***}P < 0.001$, as indicated, one-way ANOVA with Bonferroni correction.

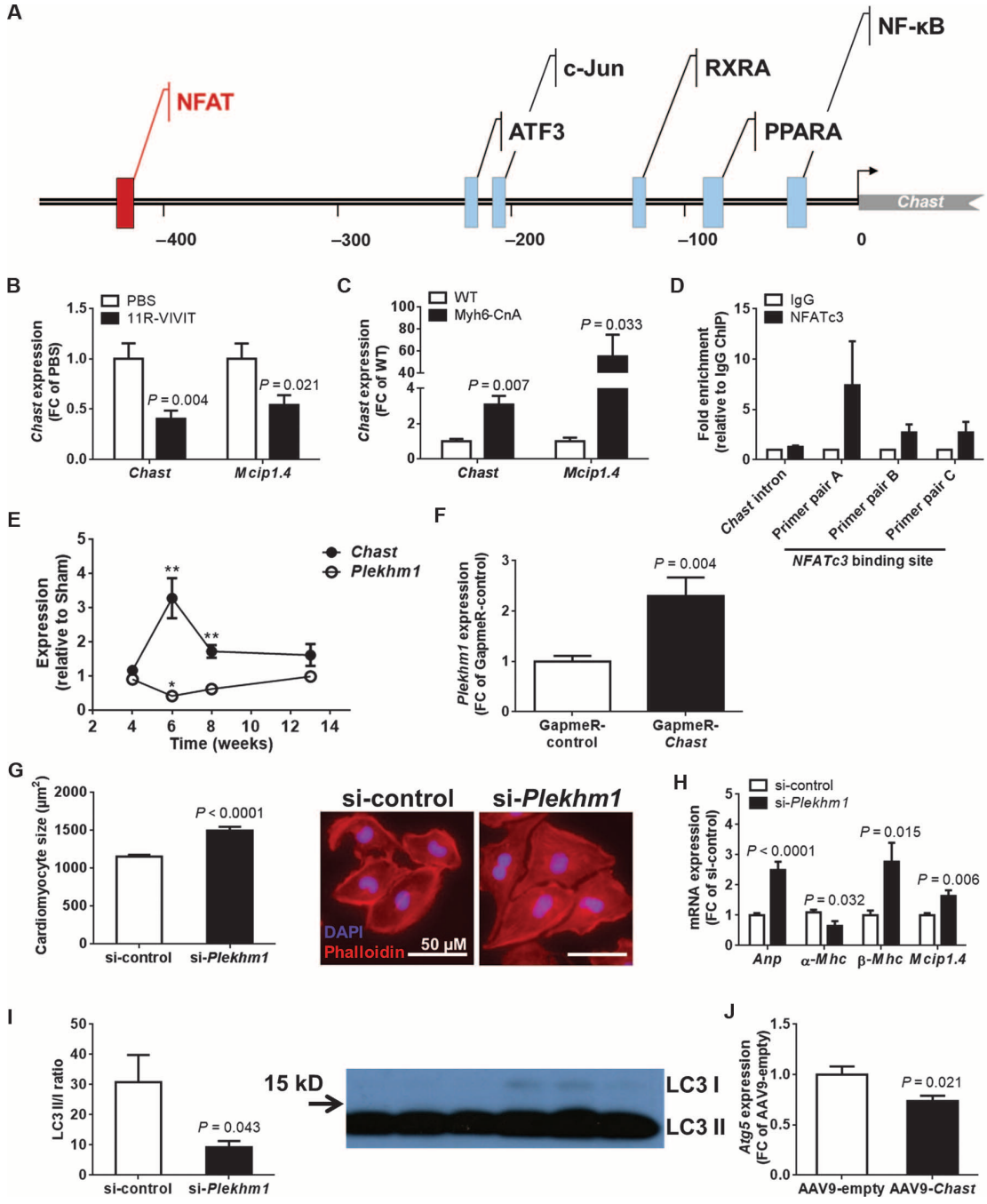

Fig. 3. Regulation of *Chast* and *Chast*-mediated regulation of *Plekhm1*. (**A**) Transcription factor binding site prediction within the genomic upstream region of the *Chast* lncRNA. ATF3, activating transcription factor 3; RXRA, retinoid × receptor α; PPARA, peroxisome proliferator-activated receptor α; NF-κB, nuclear factor κ-light-chain-enhancer of activated B cells. (**B**) *Chast* and *Mcip1.4* gene expression 2 days after treatment of mouse HL-1 cardiac muscle cells with the pharmacological NFAT inhibitor 11R-VIVIT (1 μM) or saline [phosphate-buffered saline (PBS)]. (**C**) *Chast* and *Mcip1.4* gene expression in heart tissue of calcineurin TG (Myh6-*CnA*) mice compared to wild-type (WT) littermates. Data in (B) and (C) are mean FC over PBS control ± SEM ($n \geq 3$ independent experiments; $n = 4$ mice per group). (**D**) Quantitative reverse transcription PCR (qRT-PCR) after ChIP with three different primer pairs surrounding the potential *Nfatc3* binding site in comparison to a control primer targeting the *Chast* intron. Data are mean fold enrichment relative to immunoglobulin G (IgG) control ± SEM ($n = 3$). (**E**) Time course of *Chast* and *Plekhm1* expression at different time points after TAC. Data are means ± SEM ($n = 5$ to 8). (**F**) *Plekhm1* expression in mouse HL-1 cardiomyocytes after *Chast* repression with GapmeRs. Data are means ± SEM ($n = 3$). (**G** to **I**) Cardiomyocyte size of HL-1 cells calculated from fluorescent microscopy images (G), expression of hypertrophic stress markers (H), and LC3 II/I ratios (I) after small interfering RNA (siRNA)–mediated silencing of *Plekhm1* (25 nM, for 48 hours). Data are means ± SEM ($n \geq 3$ independent experiments). (**J**) *Atg5* expression levels in hearts from mice treated with a control–AAV9 (adeno-associated virus serotype 9) vector (AAV9-empty) or an AAV9 vector overexpressing *Chast* (AAV9-*Chast*). Data are means ± SEM ($n = 6$ animals per group). In (E), $^{*}P < 0.05$; $^{**}P < 0.01$ versus 4-week time point; in all other panels, *P* value was compared to respective control; Student's *t* test.

in cytosol, nuclear soluble, and chromatin-associated forms (fig. S2), indicating that *Chast* has the ability to modulate both transcriptional and posttranscriptional processes.

Chast overlaps with two protein-coding genes, *Arhgap27* and *Plekhm1* (Fig. 1F). Expression of *Arhgap27* was not deregulated upon TAC operation or upon in vitro suppression of *Chast* using GapmeRs in HL-1 cells (fig. S3). However, upon TAC operation, *Plekhm1* expression was regulated inversely to that of *Chast* with strong down-regulation at 6 weeks after operation, corresponding to the highest expression level of *Chast* (Fig. 3E). Conversely, GapmeR-mediated silencing of *Chast* in cultured HL-1 cells resulted in a significant up-regulation of *Plekhm1* (Fig. 3F). SiRNA-mediated silencing of *Plekhm1* resulted in hypertrophic responses of cultured HL-1 cardiomyocytes (Fig. 3, G and H). These results imply that one possible mechanism of *Chast* activity is regulation of *Plekhm1*. *Plekhm1* has been shown to impede autophagy in various cell lines (*16*), and inhibition of autophagy in cardiomyocytes drives cardiac remodeling processes (*17*, *18*). Indeed, silencing of *Plekhm1* in HL-1 cells inhibited normal cardiac autophagy, as indicated by the reduction in LC3 II/I ratios (Fig. 3I). In line with this observation, hearts overexpressing *Chast* in vivo showed reduced *Atg5* levels, indicating reductions in autophagic capacity (Fig. 3J).

We next performed global microarray mRNA expression analyses after GapmeR-mediated suppression of *Chast* in murine HL-1 cardiomyocytes to get a broader insight into *Chast*-mediated transcriptome changes. *Chast* suppression affected expression of many mRNAs of the HL-1 cardiomyocyte transcriptome (fig. S4A). On the basis of two bioinformatic approaches—correlation of deregulated genes with the KEGG database (fig. S4B) and gene ontology analysis (fig. S4C)—several pathways were identified to be regulated upon *Chast* silencing: muscle development, metabolic processes, Wnt signaling, and cardiomyopathy. The deregulation of mRNAs involved in pathological cardiac pathways was validated independently by quantitative reverse transcription PRC (qRT-PCR) of HL-1 cells treated with GapmeR-*Chast* (fig. S4D). Similarly, RNA pulldown assays using biotinylated *Chast* constructs indicated that *Chast* interacts with several cardiac-relevant proteins (table S2). Pathway enrichment analysis of the interacting proteins using Enrichr revealed that *Chast* interacts mainly with proteins involved in cardiomyopathies (table S3). These bioinformatic and experimental screening tools revealed a strong correlation (as quantified by main bioinformatic hits of cardiac disease pathways rather than of others) of the lncRNA *Chast* with cardiac disease pathways, qualifying *Chast* as a potential target for therapeutics.

Chast is of translational relevance for humans

We next tested if *Chast* is conserved and regulated by prohypertrophic stimuli in humans. An alignment of the mouse *Chast* sequence to human expressed sequence tags (ESTs) revealed existence of a transcript that has a similar sequence (66% homology) and structure compared to mouse *Chast* originating from chromosome 17 (NC_000017.11| 64783199-64783552; *Homo sapiens* chr17, GRCh38.p2 Primary Assembly) (Fig. 4, A to C). We tested expression of *CHAST* and other markers of cardiac hypertrophy, as positive controls, in human embryonic stem cell (hESC)–derived cardiomyocytes. Upon treatment with a prohypertrophic stimulus (PE + ISO), human *CHAST* expression was strongly elevated, along with the other hypertrophy-responsive genes *ANP* and *MCIP1* (Fig. 4D).

Similar to murine *Chast*, overexpression of human *CHAST* in mouse HL-1 cells resulted in a significant enlargement in cardiomyocyte size showing functional conservation (Fig. 6E). *CHAST* expression was also up-regulated in hearts of patients with aortic stenosis ($n = 21$), a main direct cause for cardiac hypertrophy, compared to healthy hearts ($n = 23$) (Fig. 4F). Although preliminary, these results highlight the potential translational relevance of the *CHAST* lncRNA in human cells and tissues.

In vivo targeting of Chast ameliorates cardiac remodeling and hypertrophy

To test if prohypertrophic effects of *Chast* in cultured HL-1 cells and hESC-derived cardiomyocytes translate to therapeutic opportunities in cardiac hypertrophy, we performed in vivo gain- and loss-of-function experiments in mice. For cardiac overexpression of *Chast*, we created AAV9 viral particles where *Chast* is expressed under the control of the cardiac troponin T promoter (Fig. 5A). In vivo overexpression of *Chast* for 6 weeks induced hypertrophic growth in the mouse heart accompanied by increased cardiomyocyte size (Fig. 5, B to D). Expression of cardiac stress markers *Bnp* and β-*Mhc*, but not *Anp*, was also increased upon *Chast* overexpression (Fig. 4E). Genetic changes were accompanied by increased cardiac fibrosis as evident from picrosirius red staining (Fig. 5F) and elevated *Ctgf* (connective tissue growth factor) expression (Fig. 5G).

Consistently, Millar catheter–based measurements identified a significant increase in LV end-systolic and LV end-diastolic pressure upon *Chast* overexpression (Fig. 5H), indicating that *Chast* overexpression results in early signs of pathological remodeling processes. This is in line with increased LV pressure values in other models of pathologic cardiac hypertrophy, such as abdominal aortic banding or angiotensin II infusion (*19*, *20*). GapmeR-mediated silencing of *Chast* 1 day after TAC with weekly follow-up treatments (Fig. 6, A and B) prevented cardiac hypertrophy, keeping animals at sham levels of heart weight–to–tibia length (Fig. 6C) and cardiac stress markers *Anp* and β-*Mhc* (Fig. 6D) compared to mice treated with a scrambled control. Consistently, in vivo repression of *Chast* prevented *Plekhm1* down-regulation (Fig. 6E). Furthermore, cardiac pressure–overloaded mice treated with GapmeRs against *Chast* showed reduced fibrosis and *Ctgf* expression levels (Fig. 6, F and G), as well as improved EF (ejection fraction) and smaller systolic and diastolic volumes (Fig. 6H). The weekly dosing regimen (Fig. 6A) did not result in significant changes in clinical chemistry parameters, such as aspartate aminotransferase (AST; liver toxicity marker), cholinesterase (ChE; neurotoxicity marker), urea (kidney toxicity marker), and interleukin 6 (IL-6; a proinflammatory marker) (fig. S5).

We next tested the therapeutic potential of *Chast* inhibition in another model of established cardiac disease. Here, we treated mice 4 weeks after TAC by weekly injections of a GapmeR against a scrambled sequence (control) or against *Chast* (Fig. 7A). After 8 weeks, *Chast* inhibition led to a significant reduction in heart weight/tibia length ratios in mice compared to animals treated with control-GapmeRs (Fig. 7, B and C). This is in line with smaller cardiomyocyte sizes in histological sections of TAC animals treated with the *Chast*-GapmeR when compared with control-GapmeR treatment (Fig. 7C). Echocardiographic assessment of hearts from mice 8 weeks after TAC and treated with the control-GapmeR showed a significant decline in EF, whereas animals treated with the *Chast*-GapmeR had normal EF close to that of sham-operated animals (Fig. 7D).

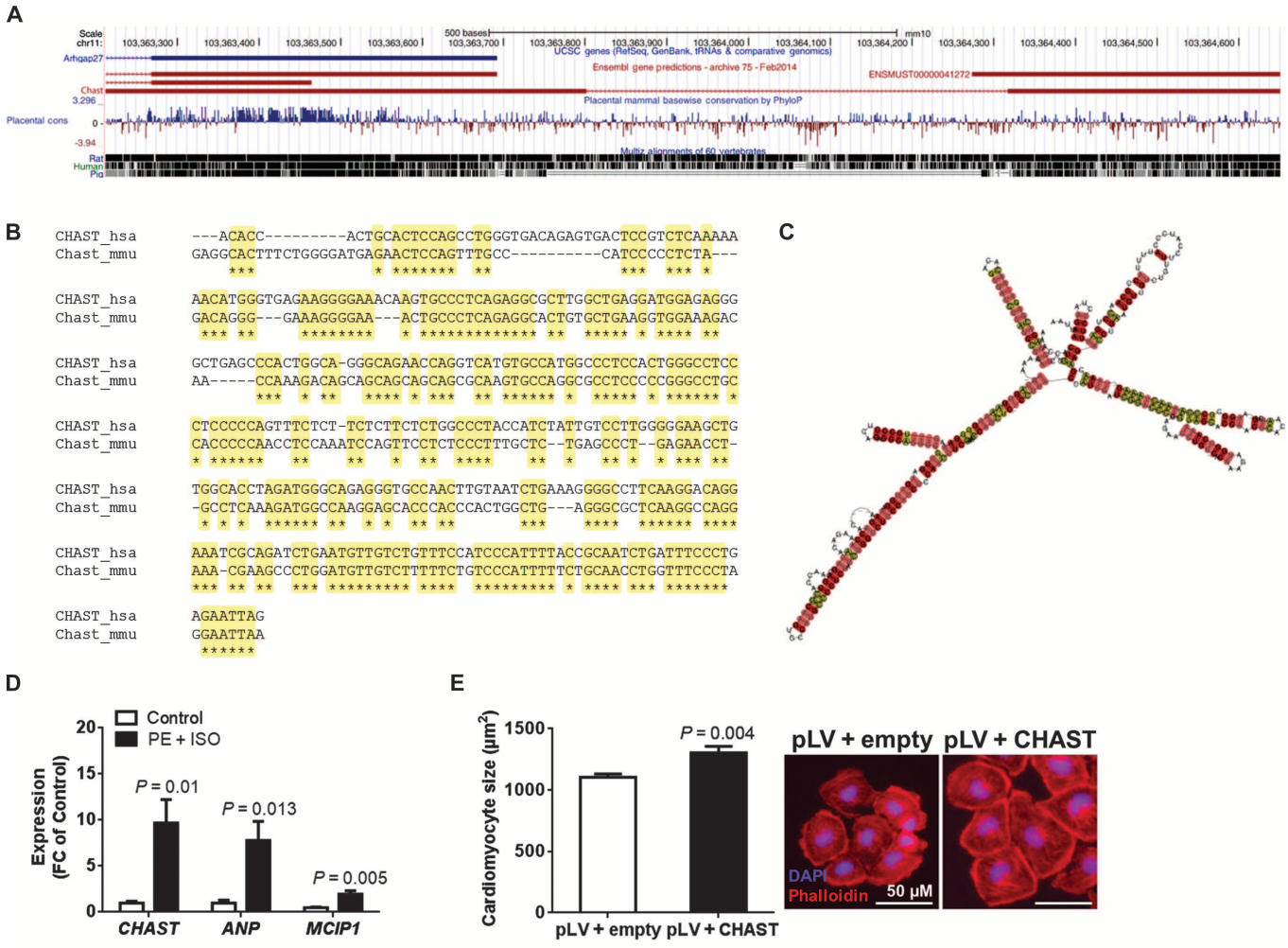

Fig. 4. *Chast* has a functional human homolog. (**A**) UCSC (University of California, Santa Cruz) Browser–derived representation of the genomic locus of *Chast* indicating conserved regions. (**B**) Pairwise alignment of the human and murine *Chast* sequence by Clustal Omega. (**C**) Consensus structure of human *CHAST* and murine *Chast* derived from LocARNA (red indicates there is only one possible pair, ochre means two possible pairs). (**D**) *CHAST* and other hypertrophic gene expression in hESC (HES3)–derived cardiomyocytes after PE and ISO treatment (10 µM each, 48 hours). Data are mean FC versus control ± SEM ($n \geq 3$ independent experiments). (**E**) HL-1 cardiomyocyte size after lentiviral overexpression of human *CHAST*. Data are means ± SEM ($n \geq 3$ independent experiments). (**F**) Expression of human *CHAST* in healthy heart tissues ($n = 23$) or in heart tissues from patients with aortic stenosis ($n = 21$). Data are mean FC versus control ± SEM. *P* values versus respective control in (D) to (F) were determined by Student's *t* test. High-resolution files for (A) and (C) are online.

DISCUSSION

Here, we present the lncRNA *Chast* as a crucial player mediating cardiac hypertrophy in vivo in mice and in vitro in murine and human cells. Targeting *Chast* by specific oligonucleotide inhibitors both prevented disease and attenuated established cardiac hypertrophy with improved heart function. Although most of the human genome is transcribed, less than 2% of it encodes for proteins. One class of noncoding RNAs, microRNAs, has been linked to several biological processes, and their translational importance has been well studied in cardiac diseases in particular. In contrast, few reports exist on the role of lncRNAs in cardiac development (*21*). One recent study identified that the lncRNA *Mhrt*, which originates from MYH7 locus, is cardioprotective, and restoration of *Mhrt* levels protects the heart from hypertrophy and failure (*22*). We have identified a new lncRNA, *Chast*, that is pro-hypertrophic in mice, demonstrates 66% homology with human *CHAST*, and can be inhibited in vivo to prevent or reverse experimental cardiac hypertrophy.

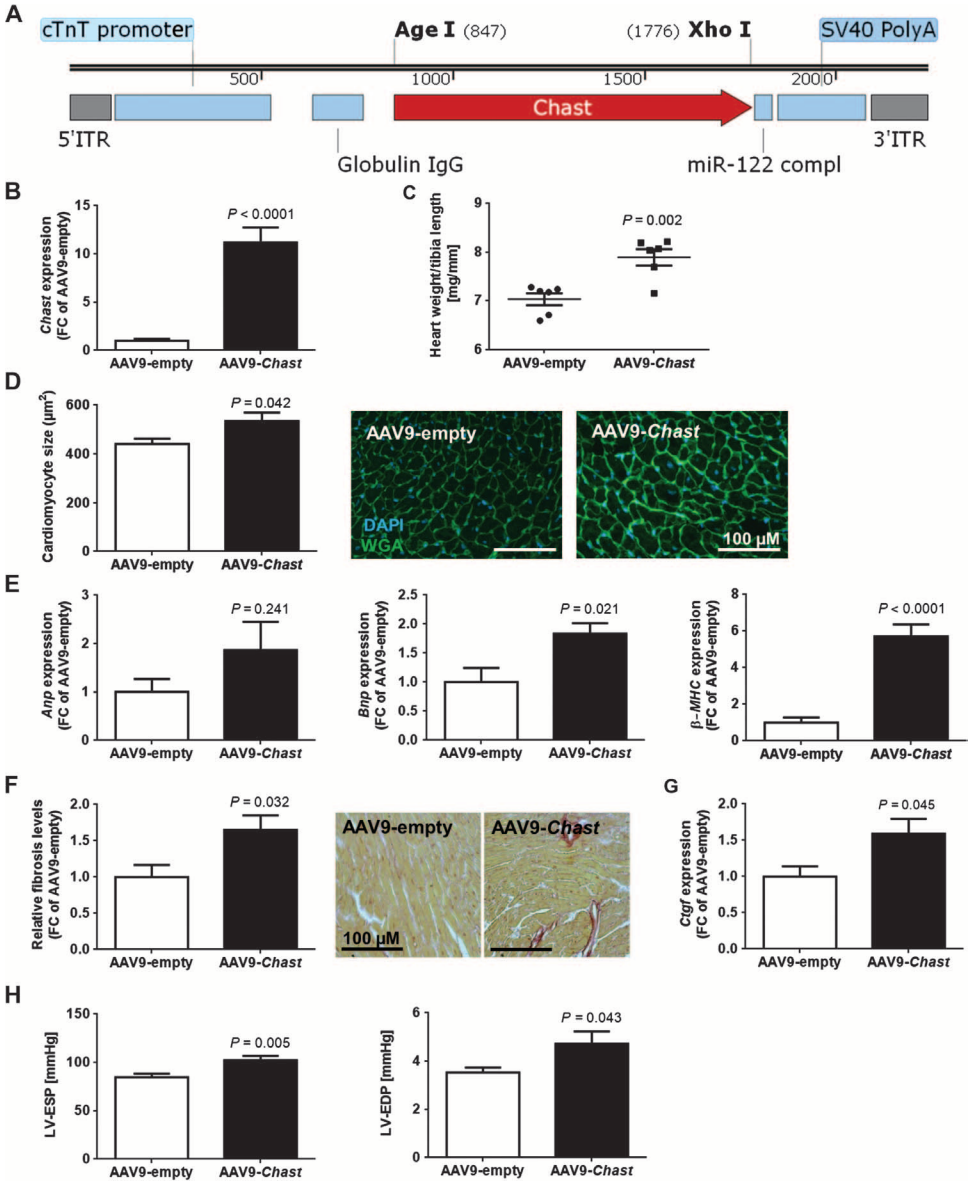

Fig. 5. In vivo overexpression of *Chast* promotes cardiac remodeling in mice. (**A**) Map of the cardiomyocyte-specific AAV9 vector. ITR, inverted terminal repeat; cTnT, cardiac troponin T promoter; miR-122 compl, miR-122 binding site (two sites). (**B**) Elevation of *Chast* levels in cardiomyocyte fraction 6 weeks after injection compared to the control virus (AAV9-empty). (**C**) Heart weight–to–tibia length ratio. Data are individual animals with means and SEM ($n = 6$). (**D**) Determination of the cardiomyocyte diameters in histological sections. WGA, wheat germ agglutinin. (**E**) Expression of hypertrophic marker genes *Anp*, *Bnp*, and β-*Mhc* after *Chast* overexpression. (**F** and **G**) Cardiac fibrosis assessed by collagen stain (picrosirius red) and (G) *Ctgf* expression. (**H**) Hemodynamic analysis of *Chast* overexpressing mice using pressure-volume catheter system (LV-ESP, left ventricular end-systolic pressure; LV-EDP, left ventricular end-diastolic pressure). Data in (B) and (D) to (H) are means ± SEM ($n = 6$ to 14). *P* values were determined by Student's *t* test.

Chast is expressed as a full-length transcript with several "stop" codons and no ORF activity, validating *Chast* as a noncoding RNA. *Chast* is not a cardiac-specific lncRNA; however, its cell type–specific expression is very sensitive to pressure overload in vivo or prohypertrophic stimuli in vitro, such as PE and ISO, in both murine and human cardiomyocytes. Consistent with this, we found that *Chast* expression was induced partly by the prohypertrophic transcription factor NFAT, leading to hypertrophic growth, as evidenced by increases in cardiac stress markers in vitro and in vivo.

LncRNAs are likely powerful treatment targets because they intensively interact with their genetic environment, placing them as crucial regulators of genetic networks. LncRNAs can function as guide strands influencing genes or proteins in trans (on distantly located genes) or in cis (on neighboring genes) (*23*). Our data reveal a potential cis-regulating role of *Chast* on the gene located on the opposite strand, named *Plekhm1*. Although our current data do not explain the exact mechanism of the *Chast*/*Plekhm1* interaction, the reciprocal regulation of both genes in disease and the direct effects of *Chast* manipulation on *Plekhm1* expression make a cis-regulatory action likely. Further studies need to show how *Chast* leads to *Plekhm1* silencing. *Plekhm1* has been recently described as a regulator of autophagy (*16*), which fits with our observation that *Plekhm1* silencing in the cardiomyocyte cell line HL-1 inhibited cardiomyocyte autophagy and drove cardiac hypertrophy. Thus, strategies overexpressing *Plekhm1* in cardiac hypertrophy–associated diseases may be of additional therapeutic relevance.

Very likely, the lncRNA *Chast* will have many more targets. For instance, bioinformatic analyses showed that *Chast* affects the transcriptome of murine HL-1 cardiomyocytes with a strong effect on pathways of cardiac muscle morphogenesis, cardiomyopathies, and Wnt signaling. Indeed, activation of Wnt signaling has been described to be an additional driver of cardiac hypertrophy (*24*). How *Chast* may affect Wnt signaling pathways as suggested by the transcriptome analyses is unknown. Additionally, our bioinformatic and mechanistic studies show that *Chast* interacts with many proteins involved in cardiac diseases, including vinculin (*25*), calmodulin (*26*), or laminins (*27*). Future studies will deepen our understanding of what additional mechanisms are involved in *Chast*'s mode of action in cardiac hypertrophy and remodeling. These studies should address how *Chast* regulates the cardiomyocyte transcriptional changes (for instance, by epigenetic processes) and what the cardiac implications of *Chast*/protein-binding events are.

GapmeR-mediated inhibition of *Chast* in pressure-overloaded mouse hearts prevented or halted hypertrophic growth, which suggests

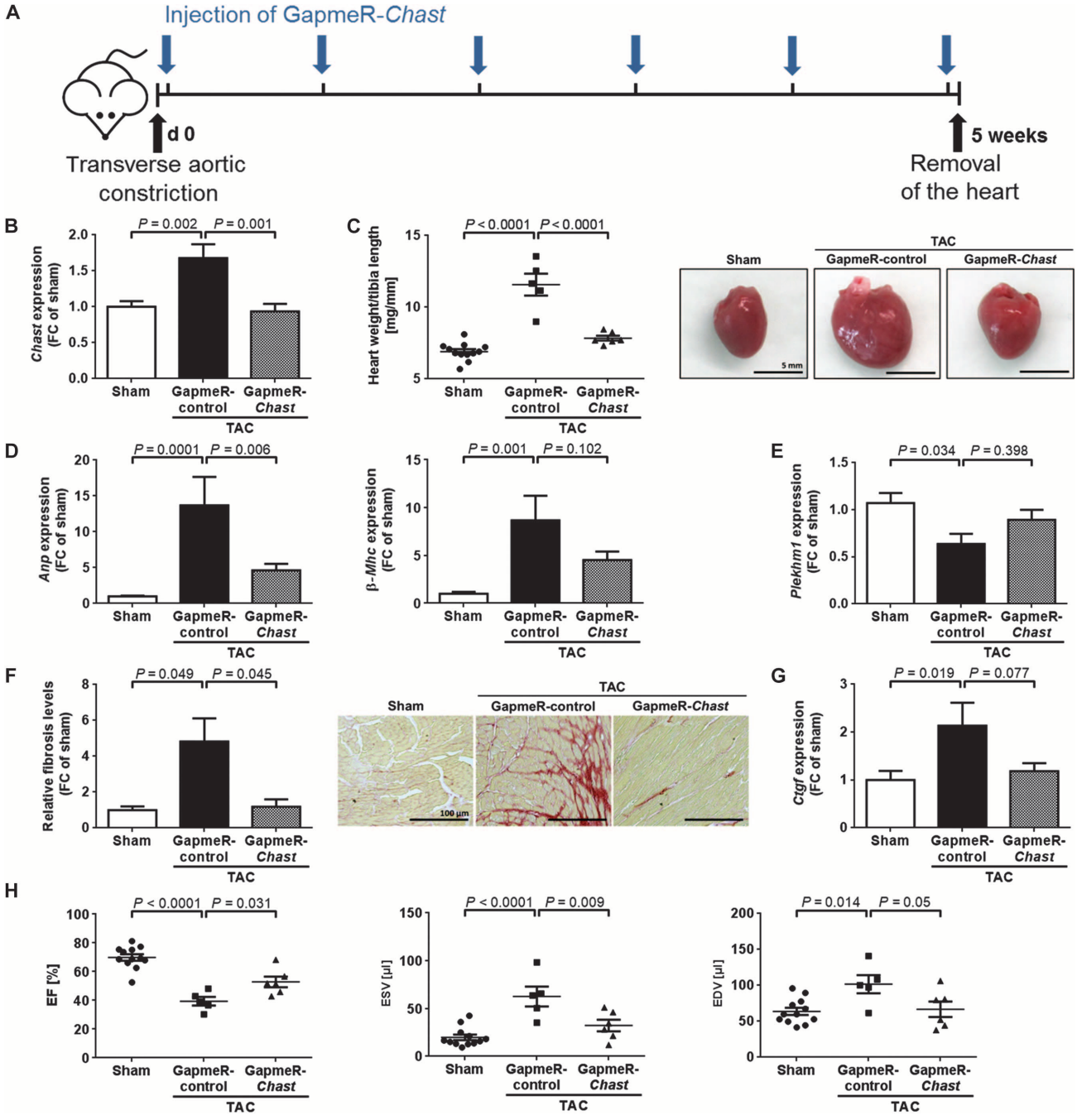

Fig. 6. Pharmacological inhibition of *Chast* in vivo prevents cardiac remodeling. (**A**) Overview of the experimental setup, where six weekly injections of GapmeR-control (negative control, scrambled sequence) or GapmeR-*Chast* were administered starting day 1 after TAC until removal of the heart at 5 weeks. D0, day 0. (**B**) Expression of *Chast* relative to sham. (**C**) Heart weight–to–tibia length ratio with representative photographs of sham- and TAC-operated mouse hearts. (**D** and **E**) Expression of hypertrophic marker genes, *Anp* and β-*Mhc* (D), as well as levels of the *Chast* antisense gene *Plekhm1* (E) relative to sham. (**F**) Cardiac fibrosis analysis and representative collagen stainings (picrosirius red). (**G**) *Ctgf* expression. (**H**) Echocardiographic analysis of cardiac dimensions and function: EF, ESV (end-systolic volume), and EDV (end-diastolic volume). Data in (B) and (D) to (G) are individual animals with means ± SEM (n = 5 to 12). Data in (C) and (H) are means ± SEM (n = 5 to 12). P values were determined by one-way ANOVA with Bonferroni correction.

that *Chast* could be a new therapeutic target for cardiomyopathies. To translate to patients, we identified a new EST in the human genome with a sequence and secondary structure similar to murine *Chast*. This homolog, *CHAST*, was significantly up-regulated in hypertrophic heart tissues from patients with aortic stenosis—but not healthy controls—and in hESC-derived cardiomyocytes after hypertrophic stimuli. This

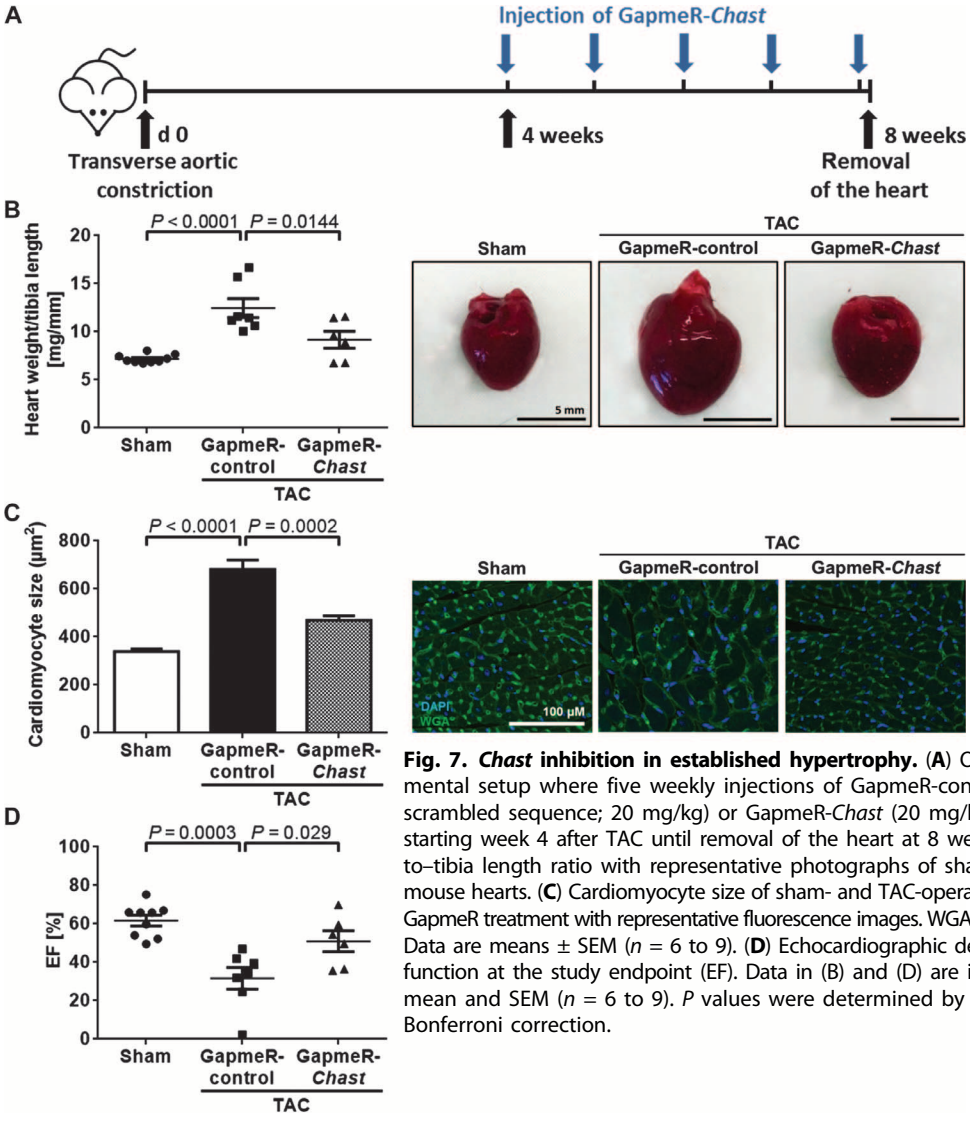

Fig. 7. *Chast* inhibition in established hypertrophy. (**A**) Overview of the experimental setup where five weekly injections of GapmeR-control (negative control, scrambled sequence; 20 mg/kg) or GapmeR-*Chast* (20 mg/kg) were administered starting week 4 after TAC until removal of the heart at 8 weeks. (**B**) Heart weight–to–tibia length ratio with representative photographs of sham- and TAC-operated mouse hearts. (**C**) Cardiomyocyte size of sham- and TAC-operated mouse hearts after GapmeR treatment with representative fluorescence images. WGA, wheat germ agglutinin. Data are means ± SEM (n = 6 to 9). (**D**) Echocardiographic determination of cardiac function at the study endpoint (EF). Data in (B) and (D) are individual animals with mean and SEM (n = 6 to 9). P values were determined by one-way ANOVA with Bonferroni correction.

is an intriguing finding because it potentially allows translation into clinical scenarios. However, there are translational hurdles to be cognizant of. Specific human *CHAST* inhibitors need to be developed and tested in human primary, hESC-derived, and/or induced pluripotent stem cell (iPSC)–derived cardiomyocytes. Because there seems to be a very high functional conservation of *CHAST* among species, as human *CHAST* drove hypertrophy in rodent cells (Fig. 4E), the next steps should be pharmacokinetic and toxicological assessments in additional animal species (rodent and nonrodent models) of *CHAST* inhibitors with the aim to test these in future clinical trials. Indeed, early toxicological evaluation of the murine *Chast* inhibitor in this study showed promising results. Intensive toxicological testing of leading *CHAST* inhibitors will be needed to search for potential adverse effects in other organs, especially the liver and kidney, because systemic toxicity affecting these organs is a primary concern in the oligonucleotide therapeutics field (*28*).

Our results highlight that *Chast* is a prohypertrophic lncRNA, and in vivo targeting of this lncRNA could be beneficial in cardiac hypertrophy. Our study sets the ground for future preclinical and clinical developments of *CHAST* inhibitors for the treatment of pathological cardiac remodeling processes, such as cardiac hypertrophy and potentially heart failure.

MATERIALS AND METHODS

Study design

The aim of this study was to identify a lncRNA that played an important role in the development of cardiac hypertrophy and to start translating these findings into a therapeutic approach. By transcriptional profiling of mouse hypertrophic hearts, we derived a lncRNA as a potential therapeutic target and performed loss- and gain-of-function studies to assess the influence of the lncRNA on the growth and genetics of murine cardiomyocytes in vitro. The TAC model using C57BL/6N mice was chosen as a well-established model of pathological cardiac hypertrophy. Real-time qPCR and measurements of the cell surface area were used to quantify cardiac hypertrophy in vitro.

Experiments were reproduced in at least three independent experiments as stated in the figure legends.

For in vivo experiments, mice were randomly assigned to treatment groups, and, wherever applicable, treatment conditions were kept blinded until statistical analysis. Group sizes were chosen on the basis of previous experiences with the TAC model, which indicated that group sizes of at least five animals could robustly identify changes in cardiac hypertrophy after at least 4 weeks of TAC. Pharmacological inhibition of the lncRNA by locked nucleic acid long RNA GapmeR injection 1 day and weekly follow-up treatments after TAC was used to illustrate the effect of in vivo repression on cardiac function and the hypertrophic gene program. In the preventive approach (weekly treatments starting at day 1 after TAC), animals were analyzed at 5 weeks, when pathological cardiac hypertrophy can be easily assessed. In the therapeutic approach (weekly treatments starting at week 4 after TAC), animals were evaluated at 8 weeks, because time was needed to establish hypertrophy by TAC before treatment started. Cardiac hypertrophy was quantified by heart weight–to–body weight or by heart weight–to–tibia length ratios, echocardiography, and qRT-PCR measurements of expression changes.

Additional studies of quantification of the human *CHAST* homolog were performed in hESC-derived cardiomyocytes treated with pro-hypertrophic stimuli. Although we used hESCs to demonstrate *CHAST* homology, cell size in hESC-derived cardiomyocytes continuously increases in culture during differentiation. Therefore, to avoid confounding influence of normal cell enlargement, we used murine HL-1 cells for the determination of *CHAST*-induced phenotype. In addition, by this experiment, we could show functional conservation of the *CHAST* sequence in other species. The effect of *CHAST* was also evaluated on cardiac tissue derived from patients with cardiac hypertrophy due to aortic stenosis or healthy human heart tissue. Aortic stenosis can be viewed as the most similar human disease to the TAC mouse model.

Animal experiments

All animal experiments were performed in accordance with the relevant guidelines and regulations with the approval of the responsible local and national authorities. To generate cardiac pressure overload, male C57BL/6N mice (8 to 10 weeks old) were subjected to TAC as described previously (*29*). Sham-operated animals underwent the same procedure without constriction of the aorta. At different time points after the surgery, as indicated in the figure captions, hearts were excised and frozen in liquid nitrogen or fractionated as described below.

Adult (8- to 10-week-old) male C57BL/6N mice were once treated by tail vein injection with 0.5×10^{12} copies of AAV9 harboring either the *Chast* sequence or an empty vector. GapmeR-*Chast* or GapmeR-negative control A (20 mg/kg) (both from Exiqon) in saline (0.9% NaCl) as carriage medium were delivered weekly by intraperitoneal injection. After 6 or 5 weeks, respectively, cardiac function and morphometric changes were assessed by echocardiography and hemodynamic measurements, and the hearts were removed for biochemical analysis. Heart tissues of calcineurin TG mice [MYH6-*CnA* (*15*)] and their wild-type littermates were provided by L.J.d.W. (Academic Hospital Maastricht, Maastricht, Netherlands).

Human tissue sampling

This study was performed with the approval of the institutional ethical committees of the University of Würzburg, Germany, and the Hannover Medical School, Hannover, Germany. We analyzed cardiac tissues from patients undergoing aortic valve replacement because of aortic stenosis (n = 21; mean age, 72.81 ± 14.61; male/female 14:7). For comparison, tissue of healthy adult human hearts was used (n = 23, mean age: 38.61 ± 12.96, male/female 14:9; hearts were donor hearts not used for transplantation or RNA from healthy human hearts was purchased from Biochain Institute). Cardiac biopsies were obtained from the left ventricle and frozen in liquid nitrogen until RNA was isolated, and gene expression measurements were performed.

Plasma sampling and biochemical analysis

EDTA-plasma samples were drawn from the mice and immediately centrifuged at 1000*g* for 10 min. The supernatant was stored at −80°C until analysis. Enzyme activities were assessed on a Modular P800 automatic analyzer using standard methods (Roche Diagnostics): AST and ChE. Urea was measured photometrically [UREAL; kinetic urease test with GLDH (glutamate dehydrogenase)] on a Cobas 6000 analyzer system (Roche Diagnostics). IL-6 levels were determined by applying the Mouse IL-6 Quantikine ELISA (enzyme-linked immunosorbent assay) Kit (R&D Systems Inc.) according to the manufacturer's protocol.

RNA isolation

Total RNA of tissues and cultured cells was isolated using RNeasy Mini Kit (Qiagen) or TriFast method (Peqlab) according to the manufacturer's instructions. Quantification and quality control were performed with Synergy HT Reader (BioTek) and Agilent 2100 Bioanalyzer (Agilent Technologies), respectively.

qRT-PCR analysis

For microarray validation and quantitative detection of lncRNAs and mRNAs, cDNAs were synthesized with the iScript Select cDNA synthesis kit (Bio-Rad), and real-time RT-qPCR analysis was performed using specific primers (table S4) and the iQ SYBR Green Mix (Bio-Rad) according to the manufacturer's protocol. Gene-specific expression levels were normalized to levels of glyceraldehyde-3-phosphate dehydrogenase (*Gapdh*) or β-actin (*ActB*).

Cell culture, transfection, and treatment

Murine HL-1 cardiomyocytes were provided by W. Claycomb (Louisiana State University Health Sciences Center, New Orleans, LA) and cultured in Claycomb medium supplemented with 10% fetal bovine serum (Sigma-Aldrich) as described (*30*). For inhibition of lncRNA function, GapmeRs (Exiqon) against specific lncRNAs were used. Cells were transiently transfected with GapmeRs (*Chast*: 5′-TGGATTTGGAGGTTGG-3′; negative control A: 5′-AACACGTCTATACGC-3′). Silencing of *Plekhm1* was achieved using 25 nM *Plekhm1* siRNA (Santa Cruz, sc-37007) and its corresponding control (Santa Cruz, sc-152320). All transfections were performed using Lipofectamine 2000 reagent (Invitrogen) according to the manufacturer's protocol.

To mimic cardiomyocyte hypertrophy in vitro, HL-1 cells were cultured in standard medium and then shifted to standard medium with low (1%) serum supplemented with 100 μM PE and 100 μM ISO (both from Sigma-Aldrich) or PBS as control. Cell exposure to the hypertrophic stimuli was stopped after 48 hours of incubation at 37°C in 5% CO_2.

In NFAT inhibition experiments, the cell-permeable peptide 11R-VIVIT (Calbiochem) at a concentration of 1 μM was added to HL-1 cells in standard medium with low serum for 48 hours.

Human pluripotent stem cells and cardiac differentiation

The hESC reporter line HES3 *MESP1*$^{mCherry/w}$/*NKX2-5*$^{eGFP/w}$ (*31*) was maintained at standard conditions on mouse embryonic fibroblasts. Cells were accutase-treated (PAA Laboratories) and seeded at the density of 0.5×10^5 cells/cm^2 on Geltrex-coated flasks in E8 medium (Stemcell Technologies) (*32*) supplemented with 10 mM Y-27632 (Tocris Bioscience) for 24 hours. Medium was replaced daily, and cells were passaged twice per week. The differentiation protocol was based on published work (*33*–*35*). Briefly, single cells were pre-inoculated on Geltrex-coated plates at 3.5×10^5 cells/cm^2 with 10 mM Y-27632 in E8. Differentiation of resulting confluent monolayer was induced 4 days after single cell seeding using the chemical Glycogen synthase kinase 3β (GSKβ) antagonist CHIR99021 (synthesized by the Institute of Organic Chemistry, Leibniz University Hannover, Hannover, Germany) at 7.5 μM for 24 hours to up-regulate Wnt-pathway activity. On day 3, the chemical Wnt-pathway inhibitor IWP2 (Tocris Bioscience) was added at 5 mM for 48 hours. During the differentiation, cells were kept in RPMI 1640 medium (Life Technologies) supplemented with B27 (without insulin). Medium was entirely replaced on days 0 (+CHIR), 1, 3 (+IWP2), and 5. Cells were cultured in RPMI 1640 supplemented with B27 from day 7 onward. For long-term maturation of cardiomyocytes, cells were cultured in RPMI 1640 supplemented with B27. Medium was replaced every 48 hours.

Assessment of cardiac differentiation efficiency was performed by flow cytometry using with the endogenous Nkx2.5-GFP reporter signal. Staining was performed as described before (*34*, *35*), applying with monoclonal antibodies targeting human troponin T, α-myosin heavy chain, and β-myosin heavy chain.

Cloning and virus production of AAV9 vectors

Chast (lncRNA ENSMUST00000130556) was synthesized and cloned into a self-complementary AAV backbone plasmid under the HEK293T control of the chicken troponin T promoter and followed by two complementary binding sites for miR-122 to minimize expression in the liver (Fig. 4A). The same plasmid lacking the Chast sequence was used as a control. Human embryonic kidney (HEK) 293 T cells were grown in 10-layer cell stacks (Thermo Scientific, 140400) for 24 hours (Dulbecco's modified Eagle's medium, 10% fetal bovine serum) before transfection. The transgene plasmid and the helper plasmid were transfected into HEK293T cells using polyethylenimine (Polysciences, 24765). After 72 hours, the viruses were harvested and purified from benzonase-treated cell lysates over an iodixanol density gradient (OptiPrep, Fresenius Kabi Norge). AAV titers were determined by real-time PCR on vector genomes using the SYBR Green Master Mix (Roche). The chicken troponin T promoter and the pDP9rs plasmid were provided by R. Hajjar (Icahn School of Medicine at Mount Sinai, New York, NY).

Fluorescence microscopy and histology

HL-1 cells were treated with 100 μM PE and 100 μM ISO (PE + ISO) as indicated in Results. For measurement of cell size, cells were fixed with 4% paraformaldehyde and stained with phalloidin–tetramethylrhodamine B isothiocyanate (10 μg/ml) and 4′,6-diamidin-2-phenylindol (DAPI) (5 μg/ml) (both from Sigma Aldrich). Cryosections of the LV myocardium were visualized by wheat germ agglutinin stain coupled to Alexa Fluor 488 (Invitrogen). The cell surface area of cardiomyocytes was calculated using the NIS-Elements BR 3.2 package (Nikon Instruments Inc.). For histological examination of fibrosis, paraffin sections of the left ventricle were stained with Sirius red and piric acid to visualize collagen deposition. The collagen content was calculated as the percentage of the area in each heart section.

Statistical analysis

For statistical analysis, GraphPad 6 (GraphPad Software) was used. Data are displayed as means ± SEM. Statistical comparison among two groups was evaluated by two-tailed unpaired Student's *t* test. For comparison of more than two groups, one-way ANOVA corrected with the Bonferroni posttest was performed. In all cases, $P < 0.05$ was considered statistically significant.

SUPPLEMENTARY MATERIALS

www.sciencetranslationalmedicine.org/cgi/content/full/8/326/326ra22/DC1
Materials and Methods
Fig. S1. *Chast* is a lncRNA.
Fig. S2. *Chast* is located in all subcellular fractions of cardiomyocytes.
Fig. S3. *Chast* does not alter *Arhgap27* levels.
Fig. S4. GapmeR-mediated silencing of *Chast* alters the transcriptome of HL-1 cells.
Fig. S5. *Chast* repression in vivo has no significant influence on plasma marker of kidney, neurological, or liver damage as well as on circulating proinflammatory IL-6 levels.
Table S1. Transcription factor binding site prediction for the *Chast* promoter.
Table S2. Cardiac relevant interaction partners enriched in the pulldown fraction of *Chast*-biotin compared to *luciferase*-biotin.
Table S3. OMIM enrichment analysis for the *Chast*-protein pulldown.
Table S4. Oligonucleotide primers used in this study.
References (*36*–*43*)

REFERENCES AND NOTES

1. J. A. Hill, E. N. Olson, Cardiac plasticity. *N. Engl. J. Med.* **358**, 1370–1380 (2008).
2. ENCODE Project Consortium, An integrated encyclopedia of DNA elements in the human genome. *Nature* **489**, 57–74 (2012).
3. J. L. Rinn, M. Kertesz, J. K. Wang, S. L. Squazzo, X. Xu, S. A. Brugmann, L. H. Goodnough, J. A. Helms, P. J. Farnham, E. Segal, H. Y. Chang, Functional demarcation of active and silent chromatin domains in human *HOX* loci by noncoding RNAs. *Cell* **129**, 1311–1323 (2007).
4. J. Feng, C. Bi, B. S. Clark, R. Mady, P. Shah, J. D. Kohtz, The *Evf-2* noncoding RNA is transcribed from the Dlx-5/6 ultraconserved region and functions as a Dlx-2 transcriptional coactivator. *Genes Dev.* **20**, 1470–1484 (2006).
5. M. Beltran, I. Puig, C. Peña, J. M. García, A. B. Álvarez, R. Peña, F. Bonilla, A. G. de Herreros, A natural antisense transcript regulates Zeb2/Sip1 gene expression during Snail1-induced epithelial–mesenchymal transition. *Genes Dev.* **22**, 756–769 (2008).
6. A. T. Willingham, A. P. Orth, S. Batalov, E. C. Peters, B. G. Wen, P. Aza-Blanc, J. B. Hogenesch, P. G. Schultz, A strategy for probing the function of noncoding RNAs finds a repressor of NFAT. *Science* **309**, 1570–1573 (2005).
7. C. M. Clemson, J. N. Hutchinson, S. A. Sara, A. W. Ensminger, A. H. Fox, A. Chess, J. B. Lawrence, An architectural role for a nuclear noncoding RNA: *NEAT1* RNA is essential for the structure of paraspeckles. *Mol. Cell* **33**, 717–726 (2009).
8. C. A. Klattenhoff, J. C. Scheuermann, L. E. Surface, R. K. Bradley, P. A. Fields, M. L. Steinhauser, H. Ding, V. L. Butty, L. Torrey, S. Haas, R. Abo, M. Tabebordbar, R. T. Lee, C. B. Burge, L. A. Boyer, *Braveheart*, a long noncoding RNA required for cardiovascular lineage commitment. *Cell* **152**, 570–583 (2013).
9. P. Grote, L. Wittler, D. Hendrix, F. Koch, S. Wahrisch, A. Beisaw, K. Macura, G. Blass, M. Kellis, M. Werber, B. G. Herrmann, The tissue-specific lncRNA *Fendrr* is an essential regulator of heart and body wall development in the mouse. *Dev. Cell* **24**, 206–214 (2013).
10. K. Wang, F. Liu, L.-Y. Zhou, B. Long, S.-M. Yuan, Y. Wang, C.-Y. Liu, T. Sun, X.-J. Zhang, P.-F. Li, A long noncoding RNA, CHRF regulates cardiac hypertrophy by targeting miR-489. *Circ. Res.* **114**, 1377–1388 (2014).
11. K. Wang, C.-Y. Liu, L.-Y. Zhou, J.-X. Wang, M. Wang, B. Zhao, W.-K. Zhao, S.-J. Xu, L.-H. Fan, X.-J. Zhang, C. Feng, C.-Q. Wang, Y.-F. Zhao, P.-F. Li, APF lncRNA regulates autophagy and myocardial infarction by targeting miR-188-3p. *Nat. Commun.* **6**, 6779 (2015).
12. K. M. Michalik, X. You, Y. Manavski, A. Doddaballapur, M. Zörnig, T. Braun, D. John, Y. Ponomareva, W. Chen, S. Uchida, R. A. Boon, S. Dimmeler, Long noncoding RNA MALAT1 regulates endothelial cell function and vessel growth. *Circ. Res.* **114**, 1389–1397 (2014).

13. R. Kumarswamy, C. Bauters, I. Volkmann, F. Maury, J. Fetisch, A. Holzmann, G. Lemesle, P. de Groote, F. Pinet, T. Thum, Circulating long noncoding RNA, LIPCAR, predicts survival in patients with heart failure. *Circ. Res.* **114**, 1569–1575 (2014).
14. L. Kong, Y. Zhang, Z.-Q. Ye, X.-Q. Liu, S.-Q. Zhao, L. Wei, G. Gao, CPC: Assess the protein-coding potential of transcripts using sequence features and support vector machine. *Nucleic Acids Res.* **35** (Suppl. 2), W345–W349 (2007).
15. J. D. Molkentin, J.-R. Lu, C. L. Antos, B. Markham, J. Richardson, J. Robbins, S. R. Grant, E. N. Olson, A calcineurin-dependent transcriptional pathway for cardiac hypertrophy. *Cell* **93**, 215–228 (1998).
16. D. G. McEwan, D. Popovic, A. Gubas, S. Terawaki, H. Suzuki, D. Stadel, F. P. Coxon, D. Miranda de Stegmann, S. Bhogaraju, K. Maddi, A. Kirchof, E. Gatti, M. H. Helfrich, S. Wakatsuki, C. Behrends, P. Pierre, I. Dikic, PLEKHM1 regulates autophagosome-lysosome fusion through HOPS complex and LC3/GABARAP proteins. *Mol. Cell* **57**, 39–54 (2015).
17. M. Taneike, O. Yamaguchi, A. Nakai, S. Hikoso, T. Takeda, I. Mizote, T. Oka, T. Tamai, J. Oyabu, T. Murakawa, K. Nishida, T. Shimizu, M. Hori, I. Komuro, T. S. Takuji Shirasawa, N. Mizushima, K. Otsu, Inhibition of autophagy in the heart induces age-related cardiomyopathy. *Autophagy* **6**, 600–606 (2010).
18. A. Ucar, S. K. Gupta, J. Fiedler, E. Erikci, M. Kardasinski, S. Batkai, S. Dangwal, R. Kumarswamy, C. Bang, A. Holzmann, J. Remke, M. Caprio, C. Jentzsch, S. Engelhardt, S. Geisendorf, C. Glas, T. G. Hofmann, M. Nessling, K. Richter, M. Schiffer, L. Carrier, L. C. Napp, J. Bauersachs, K. Chowdhury, T. Thum, The miRNA-212/132 family regulates both cardiac hypertrophy and cardiomyocyte autophagy. *Nat. Commun.* **3**, 1078 (2012).
19. A. Oláh, B. T. Németh, C. Mátyás, L. Hidi, Á. Lux, M. Ruppert, D. Kellermayer, A. A. Sayour, L. Szabo, M. Torok, A. Meltzer, L. Gellér, B. Merkely, T. Radovits, Physiological and pathological left ventricular hypertrophy of comparable degree is associated with characteristic differences of in vivo hemodynamics. *Am. J. Physiol. Heart Circ. Physiol.*, ajpheart.00588.2015 (2015).
20. H. Hermans, M. Swinnen, P. Pokreisz, E. Caluwé, S. Dymarkowski, M.-C. Herregods, S. Janssens, P. Herijgers, Murine pressure overload models: A 30-MHz look brings a whole new "sound" into data interpretation. *J. Appl. Physiol. (1985)* **117**, 563–571 (2014).
21. R. Kumarswamy, T. Thum, Non-coding RNAs in cardiac remodeling and heart failure. *Circ. Res.* **113**, 676–689 (2013).
22. P. Han, W. Li, C.-H. Lin, J. Yang, C. Shang, S. T. Nurnberg, K. K. Jin, W. Xu, C.-Y. Lin, C.-J. Lin, Y. Xiong, H.-C. Chien, B. Zhou, E. Ashley, D. Bernstein, P.-S. Chen, H.-S. V. Chen, T. Quertermous, C.-P. Chang, A long noncoding RNA protects the heart from pathological hypertrophy. *Nature* **514**, 102–106 (2014).
23. J. L. Rinn, H. Y. Chang, Genome regulation by long noncoding RNAs. *Annu. Rev. Biochem.* **81**, 145–166 (2012).
24. K. Dawson, M. Aflaki, S. Nattel, Role of the Wnt-Frizzled system in cardiac pathophysiology: A rapidly developing, poorly understood area with enormous potential. *J. Physiol.* **591**, 1409–1432 (2013).
25. A. E. Zemljic-Harpf, J. C. Miller, S. A. Henderson, A. T. Wright, A. M. Manso, L. Elsherif, N. D. Dalton, A. K. Thor, G. A. Perkins, A. D. McCulloch, R. S. Ross, Cardiac-myocyte-specific excision of the vinculin gene disrupts cellular junctions, causing sudden death or dilated cardiomyopathy. *Mol. Cell. Biol.* **27**, 7522–7537 (2007).
26. N. Yamaguchi, N. Takahashi, L. Xu, O. Smithies, G. Meissner, Early cardiac hypertrophy in mice with impaired calmodulin regulation of cardiac muscle Ca^{2+} release channel. *J. Clin. Invest.* **117**, 1344–1353 (2007).
27. J. T. Lu, A. Muchir, P. L. Nagy, H. J. Worman, *LMNA* cardiomyopathy: Cell biology and genetics meet clinical medicine. *Dis. Model. Mech.* **4**, 562–568 (2011).
28. C. L. Berman, K. Cannon, Y. Cui, D. J. Kornbrust, A. Lagrutta, S. Z. Sun, J. Tepper, G. Waldron, H. S. Younis, Recommendations for safety pharmacology evaluations of oligonucleotide-based therapeutics. *Nucleic Acid Ther.* **24**, 291–301 (2014).
29. H. A. Rockman, R. S. Ross, A. N. Harris, K. U. Knowlton, M. E. Steinhelper, L. J. Field, J. Ross Jr., K. R. Chien, Segregation of atrial-specific and inducible expression of an atrial natriuretic factor transgene in an in vivo murine model of cardiac hypertrophy. *Proc. Natl. Acad. Sci. U.S.A.* **88**, 8277–8281 (1991).
30. W. C. Claycomb, N. A. Lanson Jr., B. S. Stallworth, D. B. Egeland, J. B. Delcarpio, A. Bahinski, N. J. Izzo Jr., HL-1 cells: A cardiac muscle cell line that contracts and retains phenotypic characteristics of the adult cardiomyocyte. *Proc. Natl. Acad. Sci. U.S.A.* **95**, 2979–2984 (1998).
31. S. C. Den Hartogh, C. Schreurs, J. J. Monshouwer-Kloots, R. P. Davis, D. A. Elliott, C. L. Mummery, R. Passier, Dual reporter *MESP1*$^{mCherry/w}$-*NKX2-5*$^{eGFP/w}$ hESCs enable studying early human cardiac differentiation. *Stem Cells* **33**, 56–67 (2015).
32. G. Chen, D. R. Gulbranson, Z. Hou, J. M. Bolin, V. Ruotti, M. D. Probasco, K. Smuga-Otto, S. E. Howden, N. R. Diol, N. E. Propson, R. Wagner, G. O. Lee, J. Antosiewicz-Bourget, J. M. C. Teng, J. A. Thomson, Chemically defined conditions for human iPSC derivation and culture. *Nat. Methods* **8**, 424–429 (2011).
33. X. Lian, J. Zhang, S. M. Azarin, K. Zhu, L. B. Hazeltine, X. Bao, C. Hsiao, T. J. Kamp, S. P. Palecek, Directed cardiomyocyte differentiation from human pluripotent stem cells by modulating Wnt/β-catenin signaling under fully defined conditions. *Nat. Protoc.* **8**, 162–175 (2013).
34. H. Kempf, C. Kropp, R. Olmer, U. Martin, R. Zweigerdt, Cardiac differentiation of human pluripotent stem cells in scalable suspension culture. *Nat. Protoc.* **10**, 1345–1361 (2015).
35. H. Kempf, R. Olmer, C. Kropp, M. Rückert, M. Jara-Avaca, D. Robles-Diaz, A. Franke, D. A. Elliott, D. Wojciechowski, M. Fischer, A. Roa Lara, G. Kensah, I. Gruh, A. Haverich, U. Martin, R. Zweigerdt, Controlling expansion and cardiomyogenic differentiation of human pluripotent stem cells in scalable suspension culture. *Stem Cell Reports* **3**, 1132–1146 (2014).
36. T. D. O'Connell, M. C. Rodrigo, P. C. Simpson, Isolation and culture of adult mouse cardiac myocytes. *Methods Mol. Biol.* **357**, 271–296 (2007).
37. G. K. Smyth, Linear models and empirical bayes methods for assessing differential expression in microarray experiments. *Stat. Appl. Genet. Mol. Biol.* **3**, Article3 (2004).
38. M. T. Dittrich, G. W. Klau, A. Rosenwald, T. Dandekar, T. Müller, Identifying functional modules in protein–protein interaction networks: An integrated exact approach. *Bioinformatics* **24**, i223–i231 (2008).
39. M. J. L. de Hoon, S. Imoto, J. Nolan, S. Miyano, Open source clustering software. *Bioinformatics* **20**, 1453–1454 (2004).
40. A. J. Saldanha, Java Treeview—Extensible visualization of microarray data. *Bioinformatics* **20**, 3246–3248 (2004).
41. T. Maetzig, M. Galla, M. H. Brugman, R. Loew, C. Baum, A. Schambach, Mechanisms controlling titer and expression of bidirectional lentiviral and gammaretroviral vectors. *Gene Ther.* **17**, 400–411 (2010).
42. D. S. Cabianca, V. Casa, B. Bodega, A. Xynos, E. Ginelli, Y. Tanaka, D. Gabellini, A long ncRNA links copy number variation to a polycomb/trithorax epigenetic switch in FSHD muscular dystrophy. *Cell* **149**, 819–831 (2012).
43. V. V. Solovyev, I. A. Shahmuradov, A. A. Salamov, Identification of promoter regions and regulatory sites. *Methods Mol. Biol.* **674**, 57–83 (2010).

Acknowledgments: We thank A.S. and T.M. for help with the lentiviral lncRNA overexpression plasmid, S.E. and P.A. for the AAV constructs, A. Pich (Hannover Medical School) for the mass spectrometry analysis, as well as F.W. and L.J.d.W. for the human and murine heart tissues, respectively. We thank A. Pfanne (Hannover Medical School) for excellent technical support. Some of the healthy human heart tissues were provided by T. Kraft (Hannover Medical School). The chicken troponin T promoter and the pDP9rs plasmid were provided by R. Hajjar, Icahn School of Medicine at Mount Sinai, New York. **Funding:** The authors had support from the IFB-Tx (Integrierte Forschungs- und Behandlungszentrum Transplantation) (BMBF 01EO1302; T.T.), DFG (Deutsche Forschungsgemeinschaft) (TH 903/10-1 and RE 3523/1-1; T.T. and R.K.), the REBIRTH Excellence Cluster (T.T.), Fondation Leducq (MIRVAD; T.T.), the European Union funded ERC (European Research Council) Consolidator Grant (LONGHEART; T.T.), the Hannover Biomedical Research School program (Regenerative Sciences; T.T. and J.V.), and the Bayerische Forschungsstiftung (P.A.). R.Z. received project-related funding from the German Research Foundation (Cluster of Excellence REBIRTH DFG EXC62/3; ZW 64/4-1), the German Ministry for Education and Science (13N12606), and StemBANCC [support from the Innovative Medicines Initiative joint undertaking under grant agreement no. 115439-2, whose resources are composed of financial contribution from the European Union (FP7/2007-2013) and EFPIA (European Federation of Pharmaceutical Industries and Associations) companies' in-kind contribution]. **Author contributions:** J.V., R.K., and T.T. devised the study, designed the experiments, and wrote the manuscript. J.V. performed and analyzed all experiments with exception of the in vivo mouse studies. In vivo mouse studies were performed by A.F., K.Z., J.R., and S.B. Bioinformatic analysis and microarray evaluation were done by K.X., M.K., M.D., and T.D. Lentiviral overexpression vectors were provided by T.M. and A.S., whereas P.A. and S.E. designed and generated the adeno-associated viral constructs. Tissue samples from calcineurin TG mice and human aortic stenosis and healthy hearts were provided by L.J.d.W. and F.W., respectively. hESC-derived cardiomyocytes were prepared by E.B. and R.Z. A.J., J.F., and K.S. supported in experimental work. **Competing interests:** J.V., R.K., and T.T. have filed a patent about the diagnostic and therapeutic use of several cardiovascular lncRNAs including *Chast*/*CHAST*. **Data and materials availability:** All data and materials are available.

Submitted 17 July 2015
Accepted 27 January 2016
Published 17 February 2016
10.1126/scitranslmed.aaf1475

Citation: J. Viereck, R. Kumarswamy, A. Foinquinos, K. Xiao, P. Avramopoulos, M. Kunz, M. Dittrich, T. Maetzig, K. Zimmer, J. Remke, A. Just, J. Fendrich, K. Scherf, E. Bolesani, A. Schambach, F. Weidemann, R. Zweigerdt, L. J. de Windt, S. Engelhardt, T. Dandekar, S. Batkai, T. Thum, Long noncoding RNA *Chast* promotes cardiac remodeling. *Sci. Transl. Med.* **8**, 326ra22 (2016).

Science Translational Medicine AAAS

Long noncoding RNA *Chast* promotes cardiac remodeling

Janika Viereck, Regalla Kumarswamy, Ariana Foinquinos, Ke Xiao, Petros Avramopoulos, Meik Kunz, Marcus Dittrich, Tobias Maetzig, Karina Zimmer, Janet Remke, Annette Just, Jasmin Fendrich, Kristian Scherf, Emiliano Bolesani, Axel Schambach, Frank Weidemann, Robert Zweigerdt, Leon J. de Windt, Stefan Engelhardt, Thomas Dandekar, Sandor Batkai and Thomas Thum

(February 17, 2016)
Science Translational Medicine **8** (326), 326ra22. [doi: 10.1126/scitranslmed.aaf1475]

Editor's Summary

The missing lnc in cardiac hypertrophy

RNA that does not code for a protein comprises a large portion of the human genome. These so-called noncoding RNAs are emerging as important players in disease pathogenesis, yet their functional roles are not always well known. Viereck *et al*. have discovered a new long noncoding RNA (lncRNA) that promotes cardiac remodeling and hypertrophy in mice, which could one day be targeted with therapeutics to treat human cardiovascular diseases. The identified lncRNA, which the authors named *Chast* (for "cardiac hypertrophy–associated transcript"), was discovered to be up-regulated in hypertrophic mouse hearts. When mouse and human heart cells expressed *Chast*, they tended to be larger than their normal counterparts. By silencing *Chast* with antisense oligonucleotides, mice either did not develop hypertrophy or were rescued from established disease. In a step toward translation, the authors discovered a human homolog, *CHAST*, that similarly caused cells in a dish to enlarge. Additional investigation in patients will confirm the relevance of this lncRNA in human disease and whether it is indeed a promising target for treating cardiac hypertrophy and heart failure.

Science Translational Medicine (print ISSN 1946-6234; online ISSN 1946-6242) is published weekly, except the last week in December, by the American Association for the Advancement of Science, 1200 New York Avenue, NW, Washington, DC 20005.